Bioorganic Chemistry 84 (2019) 410–417

Contents lists available at ScienceDirect

Bioorganic Chemistry

journal homepage: www.elsevier.com/locate/bioorg

Design, synthesis and biological evaluation of novel indole derivatives as potential HDAC/BRD4 dual inhibitors and anti-leukemia agents

Gaoliang Cheng, Zhi Wang, Jinyu Yang, Yu Bao, Qihao Xu, Linxiang Zhao, Dan Liu*

Key Laboratory of Structure-Based Drugs Design & Discovery of Ministry of Education, Shenyang Pharmaceutical University, Shenyang 110016, China

ARTICLE INFO

Keywords:
HDAC and BRD4 dual inhibitor
Indole derivatives
c-Myc
Ac-H3
Anti-proliferative activity

ABSTRACT

HDAC inhibitors and BRD4 inhibitors were considered to be potent anti-cancer agents. Recent studies have demonstrated that HDAC and BRD4 participate in the regulation of some signal paths like PI3K-AKT. In this work, a series of indole derivatives that combine the inhibitory activities of BRD4 and HDAC into one molecule were designed and synthesized through the structure-based design method. Most compounds showed potent HDAC inhibitory activity and moderate BRD4 inhibitory activity. In vitro anti-proliferation activities of the synthesized compounds were also evaluated. Among them, 19f was the most potent inhibitor against HDAC3 with IC_{50} value of 5 nM and BRD4 inhibition rate of 88% at 10 μM. It was confirmed that 19f could up-regulate the expression of Ac-H3 and reduce the expression of c-Myc by western blot analysis. These results indicated that 19f was a potent dual HDAC/BRD4 inhibitor and deserved further investigation.

1. Introduction

In the past few years, epigenetic mechanisms have emerged to be relevant to a wide range of diseases including cancers, diabetes, cardiac diseases, and neurological disorders [1–4]. Lysine post-translational modification (PTM), one kind of well-studied epigenetic mechanisms, plays an extensive role in cell signaling, such as phosphorylation, methylation, acetylation and ubiquitination [5]. Acetylation level of the lysine in the N-terminal tails of histone is a vital epigenetic mark related to genes transcription [6]. Over 24,000 lysine acetylations were found in human cells which indicate that lysine acetylation plays many important roles in cell signal transduction [7]. Acetylation of the lysine is regulated by histone acetyltransferases (HATs) and histone deacetylases (HDACs) which also regarded as “writers” and “erasers”. HDACs catalyze the remove of acetyl to make the chromatin structure constrained, thereby prevent the transcription. The 18 isoforms of HDACs are grouped into four classes: class I (HDACs 1, 2, 3 and 8), class II (HDACs 4, 5, 6, 7, 9 and 10), class III (SIRT1-7) and class IV (HDAC 11) [8].

As four drugs have been approved by FDA for the treatment of lymphoma and multiple myeloma in the past eleven years, HDAC inhibitors become a promising therapy for the treatment of cancers. Vorinostat (1), also known as SAHA, was approved in 2006 by FDA as the first-in-class HDAC inhibitor for the treatment of cutaneous T-cell lymphoma (CTCL) [9]. Romidepsin, the only one ratified natural product as HDAC inhibitor, was approved in 2009 by FDA for the treatment of CTCL and peripheral T-cell lymphoma (PTCL) [10]. Belinostat (2) was approved in 2014 by the FDA to treat PTCL [11]. Panobinostat (3) was approved in 2015 by FDA as an orphan drug for the treatment of multiple myeloma (MM) [12].

Bromodomain and extra terminal (BET), another important epigenetic modulator, also participates in the regulation of genes transcription [13]. The BET family proteins can recognize acetylated lysine residues in histones H3 and H4 and thereby mediate signaling transduction [14]. The BET family is composed of bromodomain-containing protein 2 (BRD2), BRD3, BRD4, and bromodomain testis specific protein (BRDT). All the subtypes contain two N-terminal bromodomains (BD1 and BD2) and an extra C-terminal domain (ET) [15]. BRD4 was identified in 1988 as a component of the mammalian mediator complex; a coactivator plays an essential role in the regulation of transcription by RNA polymerase II (RNA Pol II) in eukaryotes [16]. BRD4 plays an important role in cellular processes, for instance, transcription, cell proliferation, differentiation and apoptosis [17]. In addition, BRD4 can enhance expression of many oncogenes, such as *c-Myc*, *Pim1* and *Bcl2*. Thus, BRD4 came to be a promising therapeutic target for cancers. Many BRD4 inhibitors have been reported in the past few years, including RVX-208, (+)-JQ1 (4), CPI-0610 (5), I-BET151 (6), and some of them are in clinical trials for the treatment of acute myelocytic leukemia (AML), MM and small cell lung cancer (SCLC) [18,19] (see Fig. 1).

Recent studies have indicated that HDAC and BRD4 are associated

* Corresponding author.
E-mail address: sammyld@163.com (D. Liu).

https://doi.org/10.1016/j.bioorg.2018.12.011
Received 14 September 2018; Received in revised form 3 December 2018; Accepted 10 December 2018
Available online 10 December 2018
0045-2068/

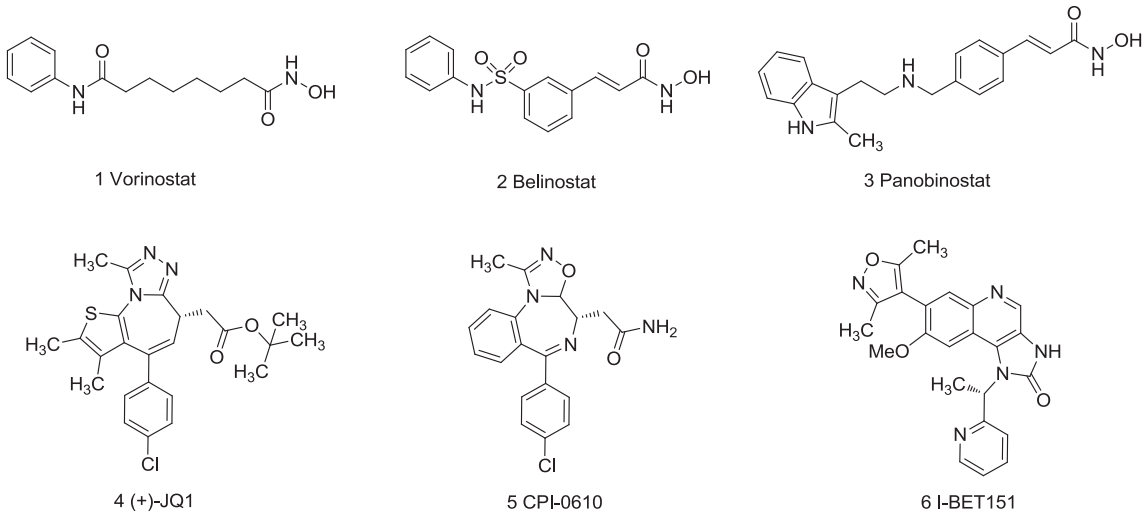

Fig. 1. Structures of some reported HDAC inhibitors and BRD4 inhibitors.

with similar biological phenotypes related to cancer and combination of the HDAC inhibitor LBH589 and BET inhibitor I-BET151 synergistically induces apoptosis of melanoma cells [20,21]. Moreover, combination of Panobinostat and (+)-JQ1 synergistically down-regulates the expression of *N-Myc* and *Bcl2* [22]. In addition, combination of Mocetinostat and (+)-JQ1 synergistically inhibits the Ras/MAPK signal pathway [23]. All these conclusions promote us to develop dual HDAC/BRD4 inhibitors.

We found the compound (7) bearing indole skeleton as HDAC inhibitor, IC_{50}(HDAC1) = 0.58 μM, IC_{50}(HDAC3) = 0.06 μM. Docking study of compound 7 and HDAC3 demonstrated that the hydroxamic group chelates the zinc ion at the bottom of the HDAC active site and the carbon chain can occupy the hydrophobic tunnel of the HDAC active site. In addition, indole skeleton and the substituent at 3-position can form hydrophobic interactions with the amino acid residues at the entrance of the HDAC active site (Fig. 2B). On the other hand, the SAR of BRD4 inhibitors have been carefully studied. Many BRD4 inhibitors consist of a hydrogen bond acceptor group as a mimic of Kac such as 3, 5-dimethylisoxazole, which interact with the conserved asparagine (Asn140), and a hydrophobic group coupled with the hydrogen bond acceptor group via a parent nucleus, which occupies the groove of WPF shelf [24–26] (Fig. 2A). It is notable that the ZA channel, a hydrophobic tunnel connects BRD4 active pocket and solvent area, is not fully occupied. Coincidently, the linker group of HDAC inhibitor is probably favorable to the ZA channel. Based on these findings, we designed and synthesized a series of compounds as candidate dual HDAC/BRD4 inhibitors. Compound 7 was taken as basic skeleton firstly. The reported BRD4 inhibitors were analysed and compound P-0014 [27] was chosen because of the similar structure to compound 7. Then the active group of BRD4 inhibitor P-0014 was introduced to basic skeleton (compound 7) to obtain the novel molecule (Fig. 2C). We hope the new molecule keeping both HDAC3 inhibitory activity and BRD4 inhibitory power.

the critical segments of both were retained and hybridized to make the new compounds' dual inhibitory activities.

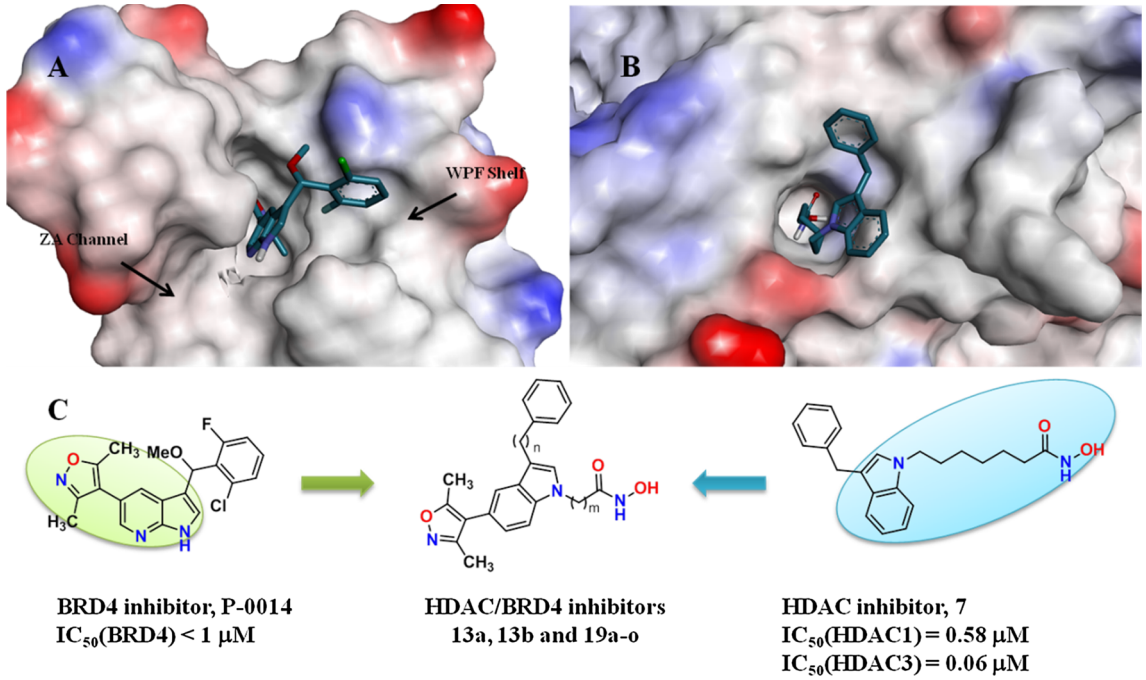

Fig. 2. (A) Binding mode of P-0014 to BRD4 (PDB ID: 5UOO); (B) Binding mode of compound 7 to HDAC3 (PDB ID: 4A69); (C) Schematic diagram of construct novel dual BRD4/HDAC inhibitors.

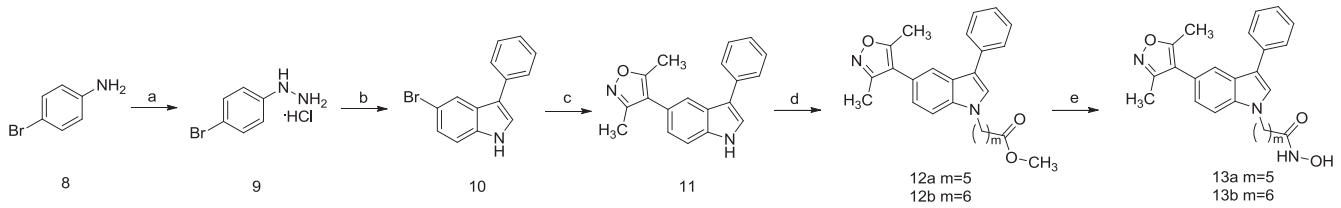

Scheme 1. Synthesis of target compounds **13a** and **13b**. Reagents and conditions: (a) $NaNO_2$, $SnCl_2$, HCl (12 mol/L), H_2O, 0 °C, 2 h; (b) phenylacetaldehyde, EtOH, reflux, 5 h; (c) 3,5-Dimethylisoxazole-4-boronic acid pinacol ester, $NaHCO_3$, Pd (dppf) Cl_2, 1,2-dimethoxyethane, H_2O, reflux, 3 h. (d) Cs_2CO_3, MeCN, reflux, 4 h; (e) NH_2OH (50 wt% in water), NaOH (2 mol/L), MeOH, r.t., 2 h.

2. Results and discussion

2.1. Chemistry

The synthetic route to target compounds 13a and 13b was illustrated as Scheme 1. 4-Bromoaniline was treated with sodium nitrite and stannous chloride in hydrochloric acid at 0 °C to give *p*-bromophenylhydrazine hydrochloride (**9**), which was reacted with phenylacetaldehyde to obtain compound **10**. Intermediate 10 was coupled with 3, 5-Dimethylisoxazole-4-boronic acid pinacol ester and the product was alkylated to give intermediate 12a and 12b. The ester groups of intermediate 12a and 12b were converted into corresponding hydroxamic acid of compounds 13a and 13b through ammonolysis.

Compounds 19a-19o were synthesized from 5-bromine indole by the route displayed in Scheme 2. 5-bromine indole was acylated at 3-position to give intermediates 15a-15h, which were hydrogenated by lithium aluminum hydride in the next step. Then the final products were synthesized from intermediates 17a-17h through coupled reaction, alkylation reaction and ammonolysis reaction successively.

2.2. In vitro HDAC and BRD4 inhibitory activity

To explore the biological activity, the HDAC inhibitory activities of novel compounds against HeLa nuclear extracts and recombinant human HDAC1, 2, 3, 6 enzymes were investigated, using Vorinostat as positive control. As shown in Table 1, all the compounds manifested inhibitory activities against class I HDACs at submicromolar concentration. However, all of them exhibited weaker activities against HDAC6 with the IC_{50} values more than 1 μM. The data indicated that these compounds were selective class I HDACs inhibitors. Ulteriorly, compound 19f showed selective HDAC3 inhibitory activity with IC_{50} of 5 nM. QSAR studies suggested that the length of the chain at 1-position of indole had a significant influence on HDAC inhibitory activity. The length with 6 carbons was more favorable for HDAC inhibitory activity than 5 carbons (exemplified by 19c and 19d). The length of the short chain at 3- position of indole also had influence on the activity. Chain length with n = 1 (19b) made the optimal value, with IC_{50} values of 0.122 μM, 0.179 μM, 0.118 μM and 0.023 μM against HDACs, HDAC1, HDAC2 and HDAC3, respectively. For the R group on the phenyl, 3-position substituted compounds demonstrated the superior HDAC inhibitory activity than 2-position and 4-position substituted compounds (exemplified by 19j, 19l and 19n). In addition, compounds with an electrophilic R group showed more potent activity than the compounds with electron-donating R group (exemplified by 19l and 19o).

All the synthesized compounds were evaluated the inhibition effects for BRD4 at 100 μM, 10 μM and 1 μM, with (+)-JQ1 as positive control. As shown in Table 1, most of them could inactive BRD4 over 50% ration at 10 μM. Compound 19f with *para*-F substitution on phenyl showed the most powerful inhibitory activity against BRD4 (88%) at 10 μM. Diversity length of the chains on 1-positon of indole were tolerable to BRD4 inhibition due to the long ZA channel in BRD4. All these results suggested that the designed compounds exhibited HDAC/BRD4 dual inhibitory activity.

2.3. Cell growth inhibition assay

The anti-proliferative effects of novel compounds were tested against THP-1 (human acute monocytic leukemia) cell line with Vorinostat and (+)-JQ1 as positive controls. The results of the anti-proliferation assay of synthesized compounds were summarized in Table 2. All the compounds showed medium potency against THP-1 cell lines. Compounds **19d** and **19o** exhibited greatest anti-proliferative activities, with GI_{50} value of 8.79 μM and 7.82 μM respectively.

2.4. Intra-cellular target validation

We then explored whether these compounds could inhibit HDAC and BRD4 in cellular condition. The levels of c-*Myc*, acetylated histone H3 (Ac-H3) and α-tubulin were determined by western blot assay in THP-1 cells treated with compound **19f** at different concentrations for 24 h. In THP-1 cell line, compound **19f** promoted acetylation of histone H3 but not α-tubulin, which proved that compound **19f** is a selective

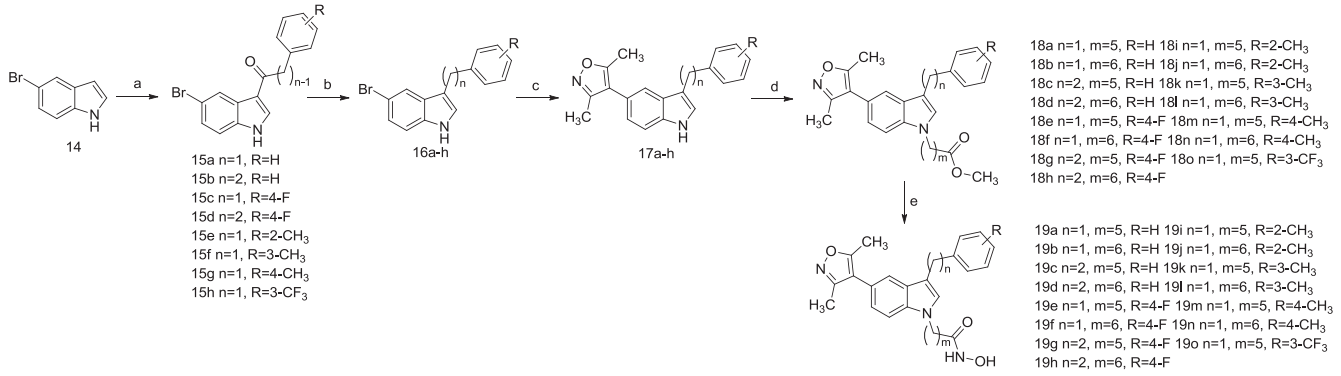

Scheme 2. Synthesis of target compounds **19a-19o**. Reagents and conditions: (a) appropriate acyl chloride, $AlCl_3$, CH_2Cl_2, r.t., 4 h; (b) $LiAlH_4$, THF, r.t., 2 h; (c) 3,5-Dimethylisoxazole-4-boronic acid pinacol ester, $NaHCO_3$, Pd (dppf) Cl_2, 1,2-dimethoxyethane, H_2O, reflux, 3 h. (d) Cs_2CO_3, MeCN, reflux, 4 h; (e) NH_2OH (50 wt% in water), NaOH (2 mol/L), MeOH, r.t., 2 h.

Table 1
The HDAC and BRD4 inhibitory activities of compounds **13a**, **13b** and **19a-19o**.[a]

Compd.	R	n	m	IC_{50} (μM)					BRD4 Inhibition Rate (%)		
				HDACs	HDAC1	HDAC2	HDAC3	HDAC6	@ 100 μM	@ 10 μM	@ 1 μM
13a	H	5	0	0.223 ± 0.031	0.260 ± 0.022	0.154 ± 0.023	0.120 ± 0.010	> 1	86	66	21
13b	H	6	0	0.183 ± 0.013	0.287 ± 0.016	0.180 ± 0.009	0.202 ± 0.012	> 1	91	76	34
19a	H	5	1	0.160 ± 0.021	0.189 ± 0.011	0.110 ± 0.012	0.089 ± 0.007	> 1	96	64	16
19b	H	6	1	0.122 ± 0.013	0.179 ± 0.011	0.118 ± 0.019	0.023 ± 0.009	> 1	96	65	31
19c	H	5	2	0.307 ± 0.019	0.247 ± 0.021	0.538 ± 0.064	0.076 ± 0.010	> 1	98	49	39
19d	H	6	2	0.172 ± 0.021	0.240 ± 0.017	0.139 ± 0.016	0.028 ± 0.005	> 1	94	64	24
19e	4-F	5	1	0.286 ± 0.034	0.341 ± 0.023	0.517 ± 0.073	0.039 ± 0.007	> 1	96	76	19
19f	4-F	6	1	0.291 ± 0.016	0.181 ± 0.011	0.298 ± 0.033	0.005 ± 0.002	> 1	95	88	28
19g	4-F	5	2	0.207 ± 0.018	0.259 ± 0.031	0.946 ± 0.086	0.017 ± 0.004	> 1	97	52	9
19h	4-F	6	2	0.030 ± 0.008	0.079 ± 0.007	0.487 ± 0.034	0.064 ± 0.007	> 1	95	50	16
19i	2-CH_3	5	1	0.369 ± 0.032	0.314 ± 0.046	> 1	0.062 ± 0.012	> 1	95	59	18
19j	2-CH_3	6	1	0.149 ± 0.009	0.220 ± 0.031	> 1	0.050 ± 0.009	> 1	97	55	14
19k	3-CH_3	5	1	0.244 ± 0.033	0.222 ± 0.019	0.568 ± 0.067	0.062 ± 0.013	> 1	94	71	15
19l	3-CH_3	6	1	0.094 ± 0.006	0.253 ± 0.012	0.127 ± 0.013	0.024 ± 0.006	> 1	96	69	14
19m	4-CH_3	5	1	0.332 ± 0.041	0.650 ± 0.053	0.956 ± 0.071	0.072 ± 0.011	> 1	97	63	18
19n	4-CH_3	6	1	0.186 ± 0.023	0.431 ± 0.033	0.438 ± 0.038	0.018 ± 0.007	> 1	95	76	13
19o	4-CF_3	6	1	0.083 ± 0.011	0.031 ± 0.005	0.079 ± 0.010	0.013 ± 0.003	> 1	92	41	12
Vorinostat				0.076 ± 0.002	0.103 ± 0.008	0.055 ± 0.007	0.027 ± 0.006	0.039 ± 0.002			
(+)-JQ1									97	96	95

[a] Each value was reproduced in three experiments.

Table 2
The anti-proliferative activities of indicated compounds and positive controls against THP-1 cell lines.[a]

Compd.	GI_{50}(μM, THP-1)	Compd.	GI_{50}(μM, THP-1)
13a	11.29 ± 1.22	**19i**	14.82 ± 0.78
13b	12.43 ± 1.63	**19j**	13.93 ± 1.23
19a	12.45 ± 2.01	**19k**	24.21 ± 2.35
19b	12.13 ± 1.39	**19l**	23.34 ± 1.87
19c	10.06 ± 0.97	**19m**	16.00 ± 2.01
19d	8.79 ± 0.65	**19n**	12.96 ± 1.42
19e	21.26 ± 2.54	**19o**	7.82 ± 0.54
19f	15.5 ± 1.23	Vorinostat	0.51 ± 0.04
19g	12.98 ± 1.35	(+)-JQ1	0.13 ± 0.02
19h	14.11 ± 2.23		

[a] Each value was reproduced in three experiments.

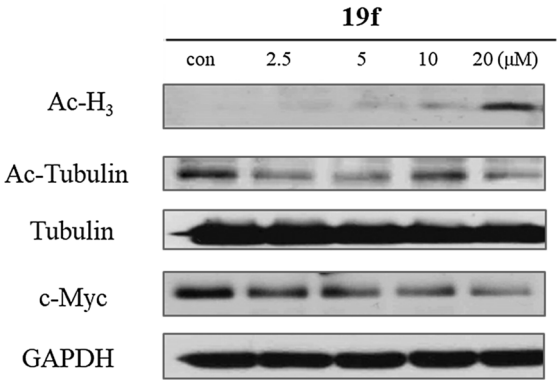

Fig. 3. Validation of HDAC and BRD4 inhibition in THP-1 cells after 24 h of treatment with compound **19f** at 2.5, 5, 10, 20 μM.

class I HDACs inhibitor. This finding is in accord with the enzyme-based assay. Moreover, the level of c-*Myc* was efficiently decreased in a dose-dependent manner (see Fig. 3).

2.5. Docking study

A docking analysis was carried out for further illustrating the possible binding modes of the synthesized compounds on HDAC and BRD4 using the Discovery Studio 3.0 software package. Compound **19f** was selected for docking evaluation as representative example and the predicted binding modes were shown in Fig. 4 below.

As illustrated by Fig. 4A and B, compound **19f** bind to HDAC3 by embedding the flexible chain into the hydrophobic tunnel and anchoring the terminal hydroxamic acid group at the bottom of the pocket. Besides the coordination with zinc ion, extra hydrogen bonds were found between the −*NH* of the hydroxamic acid group and HIS134 as well as HIS135. In addition, the indole ring of compound **19f** showed hydrophobic and van der Waals interactions with residues PHE199 and PHE200 of the receptor protein. Furthermore, the phenyl group formed a hydrophobic interaction with the residue LEU266. All these observations may explain the strong enzymatic inhibitory activity of the synthesized compounds.

The possible binding mode of compound **19f** on BRD4 was exhibited in Fig. 4C and D. The 3, 5-dimethylisoxazole group functioned as a Kac mimic and interacted with the residue ASN140 through a hydrogen bond. Moreover, a hydrogen bond was observed between the oxygen atom of the 3, 5-dimethylisoxazole group and the vicinal hydrone. In the solvent-exposed area, the hydroxamic acid group formed two hydrogen bonds with the residue PRO86. Apart from hydrogen bonding, the indole ring showed hydrophobic interactions with residues TRP81 and PRO82. Additionally, a π-π interaction was found between the phenyl group and the residue TRP81. In general, the binding modes pointed us the key interactions between synthesized compounds and the two targets which will guide us in the future design.

3. Conclusion

We reported herein a series of indole derivatives as HDAC/BRD4 dual inhibition agents. The specific structure-activity relationship of these compounds was summarized in detail simultaneously. The enzymatic assay revealed that the synthesized compounds exhibited an excellent potency of inhibiting HDAC and a good potency of inhibiting BRD4. Compound **19f** demonstrated the supreme HDAC inhibitory activity with the IC_{50} value of 5 nM and BRD4 inhibitory activity with the inhibition rate of 88% at the concentration of 10 μM. All compounds showed preferable anti-proliferation activity against human acute monocytic leukemia THP-1 cell lines with the GI_{50} value of 7.82 μM to 24.21 μM. Compound **19f** as the representative compound was used for further mechanistic studies. The results indicated that the tumor cell growth inhibitory effects were correlated with the decreased protein

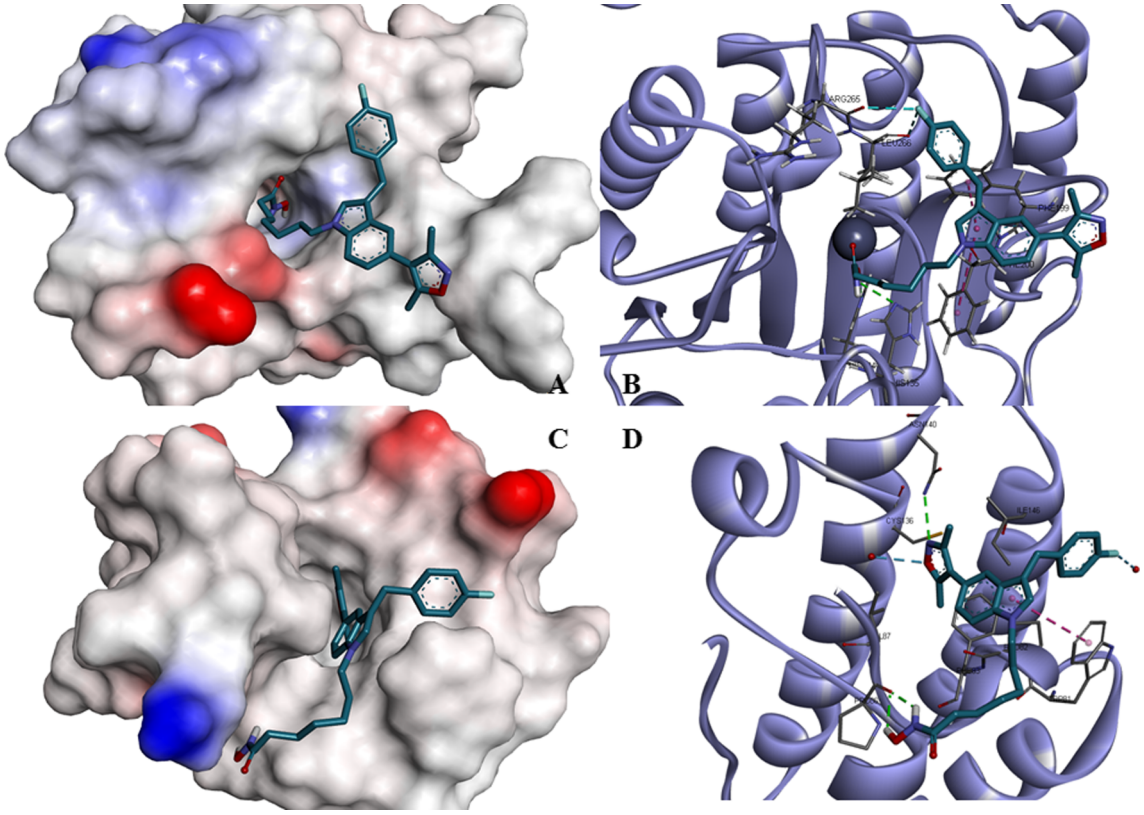

Fig. 4. Possible binding modes of **19f** to HDAC3 (A and B), BRD4 (C and D).

levels of c-*Myc* and the increased protein levels of Ac-H3. Molecular docking analysis showed that the hydroxamic acid group could form hydrogen bonds with the residues of not only HDAC but BRD4. The indole ring and the phenyl group are also essential for the key hydrophobic interactions between the compound and the targets. A novel class of HDAC/BRD4 dual inhibitors bearing indole scaffold were provided, and deserved further research.

4. Experimental

4.1. Chemistry

The melting points were determined on an electrically heated X-4 digital visual melting point apparatus and were uncorrected. Mass spectra (MS) were determined on a Finnigan MAT/USA spectrometer (LC–MS). ^{1}H NMR and ^{13}C NMR spectrum were recorded on Bruker AV-400 or ARX 600 spectrometers with tetramethylsilane (TMS) used as the internal standard. Chemical shifts were reported in ppm (δ). High–resolution mass spectra were obtained on Bruker micro TOF–Q in the ESI mode (HR–ESI–MS). All reactions were performed with commercially available reagents and they were used without further purification. All reactions were monitored by thin-layer chromatography (TLC) carried on fluorescent precoated plates GF254 (Qindao Haiyang Chemical, China) and detection of the components was made by short UV light. Column chromatography was performed with silica gel 60 (200–300 mesh).

4.1.1. General procedure for the synthesis of *13a-13b*

Material **8** (3 g, 17.4 mmol) was added to $NaNO_2$ aqueous solution (1 mol/L, 50 mL) and the mixture was stirred for 30 min at 0 °C. Then the mixture was warmed to room temperature for 90 min. A solution of $SnCl_2$ (12 g, 52.2 mmol) in concentrated hydrochloric acid (10 mL) was added dropwise to the mixture for 2 h at 0 °C. The resulting precipitate was filtered to give **9** as white solid. To a solution of **9** (2.9 g, 13.2 mmol) in ethyl alcohol (50 mL) was added hyacinthin (1.5 g, 12.5 mmol) at N_2 atmosphere and the reaction was heated to reflux for 3 h. The mixture solution was concentrated to dryness, added water (100 mL) and extracted with ethyl acetate (80 mL × 3). The organic layers were combined, washed with brine, dried with Na_2SO_4 and evaporated. Finally, the resulting residue was purified by column chromatography on silica gel as indicated to give **10** as white solid.

To a solution of **10** (0.6 g, 2.2 mmol) in glycol dimethyl ether and water mixture (30 mL, GDE: H_2O = 10:1) were added 3, 5-Dimethylisoxazole-4-boronic acid pinacol ester (0.54 g, 2.4 mmol), $NaHCO_3$ (0.56 g, 6.6 mmol) and $Pd(dppf)Cl_2$ (0.1 g, 0.1 mmol) successively at N_2 atmosphere and the reaction was warmed to 80 °C for 4 h. The mixture solution was added water (100 mL) and extracted with ethyl acetate (80 mL × 3). The organic layers were combined, washed with brine, dried with Na_2SO_4 and evaporated. Finally, the resulting residue was purified by column chromatography on silica gel as indicated to give **11** as white solid.

To a solution of **11** (0.5 g, 1.75 mmol) in acetonitrile (30 mL) were added Cs_2CO_3 (2.5 g, 5 mmol) and methyl 7-bromoheptanoate (0.44 g, 2 mmol) or methyl 6-bromohexanoate (0.42 g, 2 mmol). The reaction was warm to 70 °C for 2 h. The mixture solution was added water (50 mL) and extracted with ethyl acetate (30 mL × 3). The organic layers were combined, washed with brine, dried with Na_2SO_4 and evaporated. Finally, the resulting residue was purified by column chromatography on silica gel as indicated to give **12a or 12b** as white solid.

To a solution of **12a or 12b** (0.5 mmol) in methanol (15 mL) were added NaOH (2 mol/L, 4 mL) and NH_2OH (50 wt% in water, 3 mL) dropwise successively at 0 °C. The reaction was warmed to room temperature for 3 h. The mixture solution was concentrated to dryness, and the obtained solid was dissolved in water (10 mL). The resulting solution was adjusted to neutral with 1 mol/L aqueous solution of HCl and extracted with CH_2Cl_2 (10 mL × 3). The organic layers were combined, washed with brine, dried with Na_2SO_4 and evaporated. Finally, the

resulting residue was purified by column chromatography on silica gel as indicated to give **13a or 13b** as white solid.

*4.1.1.1. 6-(5-(3, 5-dimethylisoxazol-4-yl)-3-phenyl-1H-indol-1-yl)-N-hydroxyhexanamide (**13a**)*. Yield: 28.5%. Mp: 88.5–89.6 °C. ESI-MS: *m/z*, 416.2 $[M-H]^-$. ^{1}H NMR (600 MHz, DMSO-d_6) *δ*: 10.32 (s, 1H), 8.65 (s, 1H), 7.80 (s, 1H), 7.77 (d, *J* = 0.8 Hz, 1H), 7.68 (d, *J* = 7.1 Hz, 2H), 7.64 (d, *J* = 8.4 Hz, 1H), 7.43 (t, *J* = 7.8 Hz, 2H), 7.23 (t, *J* = 7.3 Hz, 1H), 7.18 (dd, *J* = 8.5, 1.3 Hz, 1H), 4.23 (t, *J* = 7.3 Hz, 2H), 2.40 (s, 3H), 2.22 (s, 3H), 1.95 (t, *J* = 7.4 Hz, 2H), 1.82 (dd, *J* = 15.0, 7.5 Hz, 2H), 1.56 (dd, *J* = 15.0, 7.5 Hz, 2H), 1.30 (dd, *J* = 15.0, 7.9 Hz, 2H). ^{13}C NMR (151 MHz, DMSO) *δ*: 69.40, 164.83, 158.83, 136.22, 135.54, 129.29, 127.93, 126.94, 125.91, 123.10, 121.55, 120.17, 117.42, 115.49, 111.17, 45.94, 32.51, 29.87, 26.27, 25.10, 11.67, 10.95. HRMS (ESI+) *m/z* calcd for $C_{25}H_{27}N_3O_3$ $[M-H]^-$ 416.2052 found: 416.1970.

*4.1.1.2. 7-(5-(3, 5-dimethylisoxazol-4-yl)-3-phenyl-1H-indol-1-yl)-N-hydroxyheptanamide (**13b**)*. Yield: 32.1%. Mp: 72.1–72.9 °C. ESI-MS: *m/z*, 430.1 $[M-H]^-$. ^{1}H NMR (600 MHz, DMSO-d_6) *δ*: 10.31 (s, 1H), 8.64 (d, *J* = 1.6 Hz, 1H), 7.80 (s, 1H), 7.78 (d, *J* = 1.1 Hz, 1H), 7.67 (d, *J* = 7.1 Hz, 2H), 7.64 (d, *J* = 8.5 Hz, 1H), 7.43 (t, *J* = 7.7 Hz, 2H), 7.23 (t, *J* = 7.4 Hz, 1H), 7.18 (dd, *J* = 8.4, 1.5 Hz, 1H), 4.24 (t, *J* = 7.2 Hz, 2H), 2.40 (s, 3H), 2.23 (s, 3H), 1.93 (t, *J* = 7.4 Hz, 2H), 1.81 (dd, *J* = 13.6, 6.7 Hz, 2H), 1.51–1.44 (m, 2H), 1.33–1.27 (m, 4H). ^{13}C NMR (101 MHz, DMSO) *δ*: 169.44, 164.82, 158.82, 136.24, 135.55, 129.28, 127.94, 126.91, 125.90, 123.10, 121.55, 120.19, 117.43, 115.49, 111.15, 46.03, 32.57, 30.04, 28.57, 26.43, 25.39, 11.67, 10.95. HRMS (ESI+) *m/z* calcd for $C_{26}H_{29}N_3O_3$ $[M-H]^-$ 430.2209 found: 430.2125.

*4.1.2. General procedure for the synthesis of **19a-19o***

To a mixture of $AlCl_3$ (1.5 g, 11.6 mmol) and dry CH_2Cl_2 (30 mL) was added appropriate acyl chloride (8.5 mmol) dropwise at 0 °C. Then a solution of 5-bromine indole (1.5 g, 7.6 mmol) in dry CH_2Cl_2 (20 mL) was added dropwise to the mixture for 3 h. The mixture solution was added water (50 mL) and extracted with CH_2Cl_2 (30 mL × 3). The organic layers were combined, washed with brine, dried with Na_2SO_4 and evaporated. Finally, the resulting residue was purified by column chromatography on silica gel as indicated to give **15a-15h** as light pink solid.

To a solution of **15a-15h** (4.05 mmol) in dry THF (50 mL) were added $LiAlH_4$ (0.46 g, 12 mmol) and boron fluoride ethyl ether (3 mL, 24 mmol) successively at room temperature for 1 h. The reaction was quenched by 2 mol/L aqueous solution of HCl and extracted with ethyl acetate (10 mL × 3). The organic layers were combined, washed with brine, dried with Na_2SO_4 and evaporated. Finally, the resulting residue was purified by column chromatography on silica gel as indicated to give **16a-16h** as white solid.

Compounds **19a-19o** were synthesized from **16a to 16 h** by the synthetic method from **10** to **13a** as white solid.

4.1.2.1. 6-(3-benzyl-5-(3, 5-dimethylisoxazol-4-yl)-1H-indol-1-yl)-N-hydroxyhexanamide (19a). Yield: 24.9%. Mp: 59.5–60.2 °C. ESI-MS: *m/z*, 430.2 $[M-H]^-$. ^{1}H NMR (600 MHz, DMSO-d_6) *δ*: 10.32 (s, 1H), 8.65 (dd, *J* = 7.9, 1.7 Hz, 1H), 7.49 (d, *J* = 8.5 Hz, 1H), 7.34 (d, *J* = 1.2 Hz, 1H), 7.31 (d, *J* = 7.1 Hz, 2H), 7.27 (s, 1H), 7.25 (t, *J* = 6.3 Hz, 2H), 7.14 (t, *J* = 7.3 Hz, 1H), 7.07 (dd, *J* = 8.4, 1.6 Hz, 1H), 4.12 (t, *J* = 7.1 Hz, 2H), 4.04 (s, 2H), 2.31 (s, 3H), 2.14 (s, 3H), 1.94 (t, *J* = 7.3 Hz, 2H), 1.74 (dt, *J* = 14.9, 7.3 Hz, 2H), 1.53 (dt, *J* = 15.1, 7.5 Hz, 2H), 1.29–1.24 (m, 2H). ^{13}C NMR (101 MHz, DMSO) *δ*: 169.40, 164.54, 158.72, 141.96, 134.98, 129.87, 129.55, 128.88, 128.59, 126.77, 126.05, 122.41, 119.90, 117.35, 114.00, 110.49, 48.98, 36.45, 32.50, 30.00, 28.94, 26.29, 25.11, 11.56, 10.84. HRMS (ESI+) *m/z* calcd for $C_{26}H_{29}N_3O_3$ $[M-H]^-$ 430.2209 found: 430.2078.

*4.1.2.2. 7-(3-benzyl-5-(3, 5-dimethylisoxazol-4-yl)-1H-indol-1-yl)-N-hydroxyheptanamide (**19b**)*. Yield: 23.6%. Mp: 57.8–58.3 °C. ESI-MS: *m/z*, 444.0 $[M-H]^-$. ^{1}H NMR (600 MHz, DMSO-d_6) *δ*: 10.32 (s, 1H), 8.64 (s, 1H), 7.49 (d, *J* = 8.4 Hz, 1H), 7.34 (s, 1H), 7.31 (d, *J* = 7.5 Hz, 2H), 7.26 (s, 1H), 7.25 (d, *J* = 7.8 Hz, 2H), 7.14 (t, *J* = 7.3 Hz, 1H), 7.07 (d, *J* = 10.0 Hz, 1H), 4.12 (t, *J* = 7.1 Hz, 2H), 4.04 (s, 2H), 2.31 (s, 3H), 2.14 (s, 3H), 1.92 (t, *J* = 7.4 Hz, 2H), 1.74 (dd, *J* = 13.5, 6.7 Hz, 2H), 1.49–1.43 (m, 2H), 1.28–1.24 (m, 4H). ^{13}C NMR (101 MHz, DMSO) *δ*: 169.46, 164.59, 158.84, 142.43, 135.57, 128.79, 128.53, 128.13, 126.99, 126.10, 122.47, 119.95, 119.66, 117.51, 114.14, 110.36, 45.65, 36.45, 32.59, 30.14, 28.59, 26.39, 25.39, 11.67, 10.95. HRMS (ESI+) *m/z* calcd for $C_{27}H_{31}N_3O_3$ $[M-H]^-$ 444.2365 found: 444.2222.

*4.1.2.3. 6-(5-(3, 5-dimethylisoxazol-4-yl)-3-phenethyl-1H-indol-1-yl)-N-hydroxyhexanamide (**19c**)*. Yield: 30.8%. Mp: 66.6–67.1 °C. ESI-MS: *m/z*, 444.3 $[M-H]^-$. ^{1}H NMR (600 MHz, DMSO-d_6) *δ*: 10.32 (s, 1H), 8.65 (s, 1H), 7.72 (t, *J* = 7.5 Hz, 1H), 7.49 (s, 1H), 7.27 (s, 2H), 7.26 (s, 2H), 7.19 (s, 1H), 7.17 (dd, *J* = 8.6, 4.4 Hz, 1H), 7.08 (d, *J* = 9.7 Hz, 1H), 4.10 (t, *J* = 7.0 Hz, 2H), 3.01–2.96 (m, 2H), 2.97–2.92 (m, 2H), 2.39 (s, 3H), 2.22 (s, 3H), 1.94 (d, *J* = 8.6 Hz, 2H), 1.72 (dt, *J* = 14.7, 7.2 Hz, 2H), 1.51 (d, *J* = 8.6 Hz, 2H), 1.39–1.31 (m, 2H). ^{13}C NMR (101 MHz, DMSO) *δ*: 169.37, 165.04, 158.62, 143.29, 141.61, 134.02, 130.15, 129.68, 128.93, 128.71, 128.65, 126.29, 124.95, 123.68, 116.39, 109.08, 60.96, 44.68, 32.60, 31.71, 26.28, 25.15, 11.69, 10.85. HRMS (ESI+) *m/z* calcd for $C_{27}H_{31}N_3O_3$ $[M-H]^-$ 444.2365 found: 444.2279.

*4.1.2.4. 7-(5-(3, 5-dimethylisoxazol-4-yl)-3-phenethyl-1H-indol-1-yl)-N-hydroxyheptanamide (**19d**)*. Yield: 22.1%. Mp: 70.2–71.0 °C. ESI-MS: *m/z*, 458.1 $[M-H]^-$. ^{1}H NMR (600 MHz, DMSO-d_6) *δ*: 10.32 (s, 1H), 8.65 (s, 1H), 7.50 (d, *J* = 1.4 Hz, 1H), 7.48 (d, *J* = 8.5 Hz, 1H), 7.26 (s, 2H), 7.25 (s, 2H), 7.18 (s, 1H), 7.17–7.15 (m, 1H), 7.08 (dd, *J* = 8.4, 1.6 Hz, 1H), 4.10 (t, *J* = 7.0 Hz, 2H), 3.01–2.97 (m, 2H), 2.97–2.93 (m, 2H), 2.39 (s, 3H), 2.22 (s, 3H), 1.92 (t, *J* = 7.4 Hz, 2H), 1.74–1.68 (m, 2H), 1.49–1.43 (m, 2H), 1.27–1.21 (m, 4H). ^{13}C NMR (101 MHz, DMSO) *δ*: 169.48, 164.54, 158.72, 141.97, 134.98, 129.87, 129.64, 129.55, 129.16, 128.95, 128.87, 128.80, 128.58, 127.92, 117.34, 114.00, 110.48, 48.98, 32.57, 30.38, 28.61, 26.41, 25.37, 11.57, 10.83. HRMS (ESI+) *m/z* calcd for $C_{28}H_{33}N_3O_3$ $[M-H]^-$ 458.2522 found: 458.2187.

*4.1.2.5. 6-(5-(3, 5-dimethylisoxazol-4-yl)-3-(4-fluorobenzyl)-1H-indol-1-yl)-N-hydroxyhexanamide (**19e**)*. Yield: 18.8%. Mp: 55.6–57.1 °C. ESI-MS: *m/z*, 448.0 $[M-H]^-$. ^{1}H NMR (600 MHz, DMSO-d_6) *δ*: 10.32 (s, 1H), 8.66 (s, 1H), 7.49 (d, *J* = 8.4 Hz, 1H), 7.34 (t, *J* = 2.3 Hz, 2H), 7.32 (t, *J* = 2.8 Hz, 1H), 7.27 (s, 1H), 7.08 (dd, *J* = 6.7, 2.0 Hz, 2H), 7.06 (d, *J* = 1.7 Hz, 1H), 4.14–4.10 (m, 2H), 4.03 (s, 2H), 2.32 (s, 3H), 2.15 (s, 3H), 1.93 (t, *J* = 7.3 Hz, 2H), 1.77–1.70 (m, 2H), 1.53 (p, *J* = 7.5 Hz, 2H), 1.28–1.20 (m, 3H). ^{13}C NMR (101 MHz, DMSO) *δ*: 169.35, 164.55, 158.71, 135.74, 130.58, 130.53, 127.83, 127.59, 122.47, 120.06, 119.84, 117.34, 115.29, 115.15, 113.91, 110.53, 45.65, 32.53, 30.40, 29.99, 26.30, 25.11, 11.55, 10.83. HRMS (ESI+) *m/z* calcd for $C_{26}H_{28}FN_3O_3$ $[M-H]^-$ 448.2115 found: 448.2089.

*4.1.2.6. 7-(5-(3,5-dimethylisoxazol-4-yl)-3-(4-fluorobenzyl)-1H-indol-1-yl)-N-hydroxyheptanamide (**19f**)*. Yield: 19.3%. Mp: 53.9–54.9 °C. ESI-MS: *m/z*, 462.2 $[M-H]^-$. ^{1}H NMR (600 MHz, DMSO-d_6) *δ*: 10.32 (s, 1H), 8.65 (s, 1H), 7.49 (d, *J* = 8.4 Hz, 1H), 7.34 (d, *J* = 5.9 Hz, 2H), 7.32 (d, *J* = 5.7 Hz, 1H), 7.26 (s, 1H), 7.09–7.08 (m, 1H), 7.07 (d, *J* = 2.4 Hz, 1H), 7.07–7.05 (m, 1H), 4.14–4.10 (m, 2H), 4.03 (s, 2H), 2.32 (s, 3H), 2.15 (s, 3H), 1.92 (t, *J* = 7.4 Hz, 2H), 1.73 (dt, *J* = 13.0, 6.3 Hz, 2H), 1.50–1.43 (m, 2H), 1.30–1.24 (m, 4H). ^{13}C NMR (101 MHz, DMSO) *δ*: 169.46, 164.55, 158.71, 135.75, 130.57, 130.52, 127.82, 127.59, 122.46, 120.05, 119.84, 117.34, 115.28, 115.14, 113.92, 110.52, 45.70, 32.56, 30.39, 30.12, 28.54, 26.41,

25.41, 11.56, 10.83. HRMS (ESI+) *m/z* calcd for $C_{27}H_{30}FN_3O_3$ $[M-H]^-$ 462.2271 found: 462.2182.

*4.1.2.7. 6-(5-(3, 5-dimethylisoxazol-4-yl)-3-(4-fluorophenethyl)-1H-indol-1-yl)-N-hydroxyhexanamide (**19g**)*. Yield: 22.5%. Mp: 61.0–61.3 °C. ESI-MS: *m/z*, 462.2 $[M-H]^-$. ^{1}H NMR (600 MHz, DMSO-d_6) δ: 10.32 (s, 1H), 8.66 (s, 1H), 7.49 (d, J = 2.1 Hz, 1H), 7.48 (d, J = 4.3 Hz, 1H), 7.28 (dd, J = 10.3, 3.9 Hz, 2H), 7.17 (s, 1H), 7.08 (d, J = 1.6 Hz, 1H), 7.06 (d, J = 8.9 Hz, 2H), 4.10 (t, J = 7.0 Hz, 2H), 2.99–2.95 (m, 2H), 2.95–2.91 (m, 2H), 2.39 (s, 3H), 2.22 (s, 3H), 1.93 (t, J = 7.4 Hz, 2H), 1.75–1.69 (m, 2H), 1.55–1.49 (m, 2H), 1.24–1.20 (m, 2H). ^{13}C NMR (101 MHz, DMSO) δ: 169.35, 164.59, 158.84, 135.57, 130.54, 130.49, 128.12, 127.01, 122.49, 119.97, 119.67, 117.51, 115.21, 115.08, 113.99, 110.38, 45.58, 35.60, 32.52, 30.00, 27.16, 26.26, 25.12, 11.65, 10.93. HRMS (ESI+) *m/z* calcd for $C_{27}H_{30}FN_3O_3$ $[M-H]^-$ 462.2271 found: 462.2193.

*4.1.2.8. 7-(5-(3, 5-dimethylisoxazol-4-yl)-3-(4-fluorophenethyl)-1H-indol-1-yl)-N-hydroxyheptanamide (**19h**)*. Yield: 27.1%. Mp: 78.5–79.1 °C. ESI-MS: *m/z*, 476.2 $[M-H]^-$. ^{1}H NMR (600 MHz, DMSO-d_6) δ: 10.32 (s, 1H), 8.64 (s, 1H), 7.48 (s, 1H), 7.48 (d, J = 5.2 Hz, 1H), 7.27 (dd, J = 8.6, 5.7 Hz, 2H), 7.17 (s, 1H), 7.08 (d, J = 2.3 Hz, 1H), 7.06 (dd, J = 9.2, 2.3 Hz, 2H), 4.10 (t, J = 7.0 Hz, 2H), 2.99–2.95 (m, 2H), 2.95–2.92 (m, 2H), 2.39 (s, 3H), 2.22 (s, 3H), 1.92 (t, J = 7.4 Hz, 2H), 1.74–1.68 (m, 2H), 1.49–1.43 (m, 2H), 1.23 (dd, J = 17.4, 10.3 Hz, 4H). ^{13}C NMR (101 MHz, DMSO) δ: 169.45, 164.59, 158.84, 135.57, 130.53, 130.48, 128.12, 127.04, 122.48, 119.96, 119.67, 117.51, 115.20, 115.06, 113.95, 110.36, 45.64, 35.59, 32.57, 30.13, 28.57, 27.12, 26.38, 25.37, 11.65, 10.93. HRMS (ESI+) *m/z* calcd for $C_{28}H_{33}FN_3O_3$ $[M-H]^-$ 476.2428 found: 476.2341.

*4.1.2.9. 6-(5-(3, 5-dimethylisoxazol-4-yl)-3-(2-methylbenzyl)-1H-indol-1-yl)-N-hydroxyhexanamide (**19i**)*. Yield: 32.2%. Mp: 72.1–73.1 °C. ESI-MS: *m/z*, 444.3 $[M-H]^-$. ^{1}H NMR (600 MHz, DMSO-d_6) δ: 10.31 (s, 1H), 8.65 (s, 1H), 7.49 (d, J = 8.4 Hz, 1H), 7.34 (d, J = 1.2 Hz, 1H), 7.25–7.22 (m, 1H), 7.15–7.12 (m, 1H), 7.11–7.09 (m, 2H), 7.09–7.06 (m, 2H), 4.11 (t, J = 7.0 Hz, 2H), 4.03 (s, 2H), 2.33 (s, 3H), 2.29 (s, 3H), 2.16 (s, 3H), 1.92 (t, J = 7.4 Hz, 2H), 1.75–1.69 (m, 2H), 1.54–1.48 (m, 2H), 1.23 (d, J = 3.3 Hz, 2H). ^{13}C NMR (101 MHz, DMSO) δ: 169.34, 164.53, 158.71, 139.57, 136.35, 135.68, 130.40, 129.59, 128.09, 127.82, 126.35, 126.11, 122.39, 119.97, 119.91, 117.37, 112.76, 110.50, 45.63, 32.52, 30.01, 29.22, 26.28, 25.11, 19.55, 11.60, 10.88. HRMS (ESI+) *m/z* calcd for $C_{27}H_{31}N_3O_3$ $[M-H]^-$ 444.2365 found: 444.2221.

*4.1.2.10. 7-(5-(3, 5-dimethylisoxazol-4-yl)-3-(2-methylbenzyl)-1H-indol-1-yl)-N-hydroxyheptanamide (**19j**)*. Yield: 26.5%. Mp: 77.4–78.5 °C. ESI-MS: *m/z*, 458.3 $[M-H]^-$. ^{1}H NMR (600 MHz, DMSO-d_6) δ: 10.31 (s, 1H), 8.64 (s, 1H), 7.49 (d, J = 8.4 Hz, 1H), 7.35 (d, J = 1.2 Hz, 1H), 7.25–7.21 (m, 1H), 7.15–7.12 (m, 1H), 7.11–7.09 (m, 2H), 7.09–7.06 (m, 2H), 4.11 (t, J = 7.0 Hz, 2H), 4.03 (s, 2H), 2.33 (s, 3H), 2.28 (s, 3H), 2.16 (s, 3H), 1.91 (t, J = 7.4 Hz, 2H), 1.74–1.68 (m, 2H), 1.48–1.40 (m, 2H), 1.23 (s, 4H). ^{13}C NMR (101 MHz, DMSO) δ: 169.44, 164.53, 158.71, 139.58, 136.34, 135.68, 130.41, 129.59, 128.09, 127.85, 126.36, 126.11, 122.39, 119.97, 119.92, 117.38, 112.76, 110.49, 45.67, 32.57, 30.12, 29.22, 28.55, 26.40, 25.42, 19.54, 11.61, 10.88. HRMS (ESI+) *m/z* calcd for $C_{28}H_{33}N_3O_3$ $[M-H]^-$ 458.2522 found: 458.2438.

*4.1.2.11. 6-(5-(3, 5-dimethylisoxazol-4-yl)-3-(3-methylbenzyl)-1H-indol-1-yl)-N-hydroxyhexanamide (**19k**)*. Yield: 25.2%. Mp: 69.3–70.7 °C. ESI-MS: *m/z*, 444.2 $[M-H]^-$. ^{1}H NMR (600 MHz, DMSO-d_6) δ: 10.32 (s, 1H), 8.65 (s, 1H), 7.48 (d, J = 8.4 Hz, 1H), 7.36 (s, 1H), 7.26 (s, 1H), 7.13 (d, J = 7.2 Hz, 2H), 7.10 (d, J = 7.8 Hz, 1H), 7.07 (dd, J = 8.4, 1.5 Hz, 1H), 6.96 (d, J = 7.5 Hz, 1H), 4.12 (t, J = 7.1 Hz, 2H), 3.99 (s, 2H), 2.32 (s, 3H), 2.24 (s, 3H), 2.15 (s, 3H), 1.93 (t, J = 7.4 Hz, 2H), 1.74 (dt, J = 14.7, 7.3 Hz, 2H), 1.52 (dd, J = 14.8, 7.4 Hz, 2H), 1.28–1.24 (m, 2H). ^{13}C NMR (101 MHz, DMSO) δ: 169.35, 164.52, 158.70, 141.88, 137.54, 135.70, 129.52, 128.48, 127.95, 127.47, 127.28, 126.69, 126.01, 122.37, 119.94, 117.35, 114.08, 110.48, 45.64, 32.53, 31.28, 30.00, 26.30, 25.12, 21.38, 11.56, 10.84. HRMS (ESI+) *m/z* calcd for $C_{27}H_{31}N_3O_3$ $[M-H]^-$ 445.2365 found: 444.2287.

*4.1.2.12. 7-(5-(3, 5-dimethylisoxazol-4-yl)-3-(3-methylbenzyl)-1H-indol-1-yl)-N-hydroxyheptanamide (**19l**)*. Yield: 23.7%. Mp: 59.0–59.6 °C. ESI-MS: *m/z*, 458.4 $[M-H]^-$. ^{1}H NMR (600 MHz, DMSO-d_6) δ: 10.32 (s, 1H), 8.64 (s, 1H), 7.48 (d, J = 8.4 Hz, 1H), 7.37 (s, 1H), 7.26 (s, 1H), 7.14 (t, J = 7.4 Hz, 2H), 7.10 (d, J = 7.6 Hz, 1H), 7.07 (dd, J = 8.4, 1.1 Hz, 1H), 6.96 (d, J = 7.3 Hz, 1H), 4.12 (t, J = 6.9 Hz, 2H), 3.99 (s, 2H), 2.33 (s, 3H), 2.23 (s, 3H), 2.16 (s, 3H), 1.92 (t, J = 7.4 Hz, 2H), 1.74 (dd, J = 13.0, 6.7 Hz, 2H), 1.46 (dd, J = 13.9, 6.8 Hz, 2H), 1.26 (d, J = 2.6 Hz, 4H). ^{13}C NMR (101 MHz, DMSO) δ: 169.44, 164.52, 158.71, 141.90, 137.54, 135.69, 129.51, 128.47, 127.95, 127.50, 127.28, 126.69, 126.00, 122.37, 119.94, 117.35, 114.08, 110.47, 45.68, 32.57, 31.26, 30.13, 28.57, 26.43, 25.42, 21.38, 11.56, 10.85. HRMS (ESI+) *m/z* calcd for $C_{28}H_{33}N_3O_3$ $[M-H]^-$ 459.2522 found: 458.2470.

*4.1.2.13. 6-(5-(3, 5-dimethylisoxazol-4-yl)-3-(4-methylbenzyl)-1H-indol-1-yl)-N-hydroxyhexanamide (**19m**)*. Yield: 24.3%. Mp: 61.3–62.2 °C. ESI-MS: *m/z*, 444.3 $[M-H]^-$. ^{1}H NMR (600 MHz, DMSO-d_6) δ: 10.32 (s, 1H), 8.66 (s, 1H), 7.48 (d, J = 8.4 Hz, 1H), 7.32 (s, 1H), 7.23 (s, 1H), 7.18 (d, J = 7.6 Hz, 2H), 7.06 (d, J = 7.8 Hz, 3H), 4.11 (s, 3H), 3.99 (s, 2H), 2.32 (s, 3H), 2.23 (s, 3H), 2.15 (s, 3H), 1.93 (s, 2H), 1.73 (s, 2H), 1.52 (s, 2H), 1.25 (s, 3H). ^{13}C NMR (101 MHz, DMSO) δ: 169.35, 164.52, 158.71, 145.64, 138.83, 135.72, 134.93, 130.11, 129.98, 129.14, 128.79, 122.38, 119.92, 117.36, 114.25, 110.46, 45.63, 32.53, 30.92, 30.01, 26.30, 25.11, 20.95, 11.55, 10.83. HRMS (ESI+) *m/z* calcd for $C_{27}H_{31}N_3O_3$ $[M-H]^-$ 444.2365 found: 444.2281.

*4.1.2.14. 7-(5-(3, 5-dimethylisoxazol-4-yl)-3-(4-methylbenzyl)-1H-indol-1-yl)-N-hydroxyheptanamide (**19n**)*. Yield: 21.1%. Mp: 65.5–66.0 °C. ESI-MS: *m/z*, 458.0 $[M-H]^-$. ^{1}H NMR (600 MHz, DMSO-d_6) δ: 10.32 (s, 1H), 8.64 (d, J = 1.1 Hz, 1H), 7.48 (d, J = 8.4 Hz, 1H), 7.32 (d, J = 1.0 Hz, 1H), 7.23 (s, 1H), 7.18 (d, J = 7.9 Hz, 2H), 7.06 (d, J = 7.6 Hz, 3H), 4.11 (t, J = 7.2 Hz, 2H), 3.99 (s, 2H), 2.32 (s, 3H), 2.23 (s, 3H), 2.15 (s, 3H), 1.92 (t, J = 7.3 Hz, 2H), 1.73 (dd, J = 13.5, 6.7 Hz, 2H), 1.49–1.42 (m, 2H), 1.29–1.24 (m, 4H). ^{13}C NMR (101 MHz, DMSO) δ: 169.46, 164.52, 158.71, 145.64, 138.84, 135.72, 134.93, 130.11, 129.97, 129.13, 128.78, 122.37, 119.92, 117.36, 114.26, 110.45, 45.68, 32.57, 30.91, 30.13, 28.55, 26.41, 25.41, 20.95, 11.55, 10.83. HRMS (ESI+) *m/z* calcd for $C_{28}H_{33}N_3O_3$ $[M-H]^-$. 458.2522 found: 458.2446.

*4.1.2.15. 7-(5-(3, 5-dimethylisoxazol-4-yl)-3-(3-(trifluoromethyl)benzyl)-1H-indol-1-yl)-N-hydroxyheptanamide (**19o**)*. Yield: 18.9%. Mp: 57.2–58.1 °C. ESI-MS: *m/z*, 512.1 $[M-H]^-$. ^{1}H NMR (600 MHz, DMSO-d_6) δ: 10.32 (s, 1H), 8.65 (s, 1H), 7.68 (s, 1H), 7.63 (d, J = 6.9 Hz, 1H), 7.51 (s, 2H), 7.49 (s, 1H), 7.39 (s, 1H), 7.35 (s, 1H), 7.08 (dd, J = 8.4, 1.5 Hz, 1H), 4.15 (s, 2H), 4.13 (t, J = 7.1 Hz, 2H), 2.31 (s, 3H), 2.13 (s, 3H), 1.91 (d, J = 7.7 Hz, 2H), 1.76–1.71 (m, 2H), 1.51–1.47 (m, 2H), 1.25 (d, J = 7.0 Hz, 4H). ^{13}C NMR (101 MHz, DMSO) δ: 169.41, 164.54, 158.69, 143.68, 135.67, 133.07, 129.62, 127.83, 127.76, 125.18, 122.86, 122.54, 120.18, 119.77, 117.31, 113.20, 110.60, 45.72, 35.49, 32.79, 30.09, 28.88, 28.04, 27.61, 25.31, 19.03, 11.49, 10.77. HRMS (ESI+) *m/z* calcd for $C_{28}H_{30}F_3N_3O_3$ $[M-H]^-$ 512.2239 found: 512.2143.

4.2. Biological assays

4.2.1. HDAC inhibition fluorescence assay

In this HDACs assay, HeLa nuclear extracts (Enzo Life Sciences,

USA) were used as a source of histone deacetylase. The recombinant human HDAC1, 2, 3 and 6 were purchased from BPS Bioscience (USA). All reactions were performed in the black half area 96–well microplates. A serial dilution of the inhibitors (5 μL/well) and enzymes (5 μL/well) were pre-incubated in HDAC buffer (10 μL/well) at 25 °C for 15 min, and then fluorogenic substrate (5 μL/well) Boc–Lys(Ac)–AMC was added. After incubation at 37 °C for 60 min, the mixture was stopped by the addition of developer (25 μL/well) for 10 min. Fluorescence intensity was measured using the Thermo Scientific Varioskan Flash Station at excitation and emission wavelengths of 355 (or 360 for the HeLa NuEx) and 460 nm, respectively. The IC_{50} values were extracted by curve fitting the dose/response slopes.

4.2.2. BRD4 inhibition HTFR assay

In this BRD4 inhibition assay, BRD4(1/2) GST-tag (BPS Bioscience, USA) was used as a source of bromodomain, [Lys(5,8,12,16)Ac] H4(1–21) biotinylated peptide was used as a source of histone peptide and EPIgeneous Binding Domain Kit C was used as detection reagents. All reactions were performed in the 384-well small volume plates. BRD4(1/2) GST-tag (4 μL/well), a serial dilution of the inhibitors (2 μL/well), biotin-peptide (2 μL/well), streptavidin-acceptor (5 μL/well) and anti GST-donor Ab (5 μL/well) were added successively. The reaction was incubated for 3 h at room temperature. Fluorescence emission at 665 nm and 620 nm wavelengths were measured using the Thermo Scientific Varioskan Flash Station, respectively. The IC_{50} values were extracted by curve fitting the dose/response slopes.

4.2.3. Anti-proliferative assays

Cells were provided by the Shanghai Cell Bank, Chinese Academy of Sciences. The cells were cultured in media, RMPI-1640 with 10% FBS and antibiotics (100 units/mL penicillin G sodium and 100 ng/mL streptomycin). All cells were incubated in a Thermo/Forma Scientific CO_2 water jacketed incubator with 5% CO_2 in air at 37 °C. The anti-proliferative activities of target compounds were evaluated by cytometry. Cells (2×10^5 cells/well in 100 μL medium) were incubated for 24 h then various concentrations of each compound mixed in 100 μL medium were added to each well. After another 72 h of incubation at 37 °C, The viable cells were measured using Trypan Blue reagents following manufacturer's instructions, and the % viable cells were calculated by comparing to no-drug controls. Dose-response curves were plotted in GraphPad Prism and fitted using sigmoidal nonlinear regression to determine pGI_{50} values.

4.2.4. Western blot assays

The human leukemia cell line THP-1 cells were incubated in presence of the test compound **19f** (in 0.5% DMSO) for 24 h or 48 h, harvested, and rinsed with ice-cold PBS.Total protein extracts (40 μg) were prepared by lysing cells in RIPA buffer (50 mM Tris-HCl, pH 8.0 0.5% sodium deoxycholate, 100 μM leupeptin, 2 μg/mL aprotinin, 150 mM NaCl, 1% NP-40, 0.1% SDS and 1 mM phenylmethylsulfonyl fluoride). Protein concentrations in the lysates were determined using a Bio-Rad protein assay kit (Bio–Rad Laboratories Inc., Hercules, CA, USA) according to the manufacturer's instructions. The samples were separated on SDS polyacrylamide gels and then transferred to nitrocellulose membranes and blocked with 5% nonfat dried milk. The membranes were incubated with antibodies to Ac-H3, α-tubulin, Ac-tubulin, c-Myc, Bcl-2 and β-actin overnight at 4 °C. The immune-complexes were visualized using enhanced chemiluminescence western blot detection reagents (Amersham Biosciences Inc., Piscataway, NJ).

Acknowledgment

This work was supported by the National Nature Science Foundation of China (No. 81473086).

References

[1] E. Dirice, R.W.S. Ng, R. Martinez, J. Hu, F.F. Wagner, E.B. Holson, B.K. Wagner, R.N. Kulkarni, Isoform-selective inhibitor of histone deacetylase 3 (HDAC3) limits pancreatic islet infiltration and protects female nonobese diabetic mice from diabetes, J. Biol. Chem. 292 (2017) 17598–17608.
[2] W.W. Blakeslee, K.M. Demos-Davies, D.D. Lemon, K.M. Lutter, M.A. Cavasin, S. Payne, K. Nunley, C.S. Long, T.A. McKinsey, S.D. Miyamoto, Histone deacetylase adaptation in single ventricle heart disease and a young animal model of right ventricular hypertrophy, Pediatr. Res. 82 (2017) 642–649.
[3] L. Mahady, M. Nadeem, M. Malek-Ahmadi, K. Chen, S.E. Perez, E.J. Mufson, Frontal cortex epigenetic dysregulation during the progression of Alzheimer's disease, J. Alzheimers Dis. 62 (2018) 115–131.
[4] J. Hu, Y. Wang, Y. Li, D. Cao, L. Xu, S. Song, M.S. Damaneh, J. Li, Y. Chen, X. Wang, L. Chen, J. Shen, Z. Miao, B. Xiong, Structure-based optimization of a series of selective BET inhibitors containing aniline or indoline groups, Eur. J. Med. Chem. 150 (2018) 156–175.
[5] C.H. Arrowsmith, C. Bountra, P.V. Fish, K. Lee, M. Schapira, Epigenetic protein families: a new frontier for drug discovery, Nat. Rev. Drug Discov. 11 (2012) 384–400.
[6] A.M.A. Aboeldahab, E.A.M. Beshr, M.E. Shoman, S.M. Rabea, O.M. Aly, Spirohydantoins and 1,2,4-triazole-3-carboxamide derivatives as inhibitors of histone deacetylase: design, synthesis, and biological evaluation, Eur. J. Med. Chem. 146 (2018) 79–92.
[7] T. Kouzarides, Acetylation: a regulatory modification to rival phosphorylation, EMBO J. 19 (2000) 1176–1179.
[8] S.W. Chao, L.C. Chen, C.C. Yu, C.Y. Liu, T.E. Lin, J.H. Guh, C.Y. Wang, C.Y. Chen, K.C. Hsu, W.J. Huang, Discovery of aliphatic-chain hydroxamates containing indole derivatives with potent class I histone deacetylase inhibitory activities, Eur. J. Med. Chem. 143 (2018) 792–805.
[9] A.T. Negmeldin, J.R. Knoff, M.K.H. Pflum, The structural requirements of histone deacetylase inhibitors: C4-modified SAHA analogs display dual HDAC6/HDAC8 selectivity, Eur. J. Med. Chem. 143 (2018) 1790–1806.
[10] L.P.H. Yang, Romidepsin in the treatment of T-cell lymphoma, Drugs 71 (2011) 1469–1480.
[11] R.M. Poole, Belinostat: first global approval, Drugs 74 (2014) 1543–1554.
[12] K.P. Garnock-Jones, Panobinostat: first global approval, Drugs 75 (2015) 695–704.
[13] J. Li, P. Wang, B. Zhou, J. Shi, J. Liu, X. Li, L. Fan, Y. Zheng, L. Ouyang, Development of 4,5-dihydro-benzodiazepinone derivatives as a new chemical series of BRD4 inhibitors, Eur. J. Med. Chem. 121 (2016) 294–299.
[14] Z. Liu, P. Wang, H. Chen, E.A. Wold, B. Tian, A.R. Brasier, J. Zhou, Drug discovery targeting bromodomain-containing protein 4, J. Med. Chem. 60 (2017) 4533–4558.
[15] C. Dhalluin, J.E. Carlson, L. Zeng, C. He, A.K. Aggarwal, M.M. Zhou, Structure and ligand of a histone acetyltransferase bromodomain, Nature 399 (1999) 491–496.
[16] Y.W. Jiang, H. Erdjument-Bromag, P. Temps, J.W. Conaway, R.C. Conawa, R.D. Kornberg, Mammalian mediator of transcriptional regulation and its possible role as an end-point of signal transduction pathways, Proc. Natl. Acad. Sci. USA 95 (1998) 8538–8543.
[17] E. Tonouchi, Y. Gen, T. Muramatsu, H. Hiramoto, K. Tanimoto, J. Inoue, J. Inazawa, miR-3140 suppresses tumor cell growth by targeting BRD4 via its coding sequence and downregulates the BRD4-NUT fusion oncoprotein, Sci. Rep. 8 (2018) 4482.
[18] S. Picaud, C. Wells, I. Felletar, D. Brotherton, S. Martin, P. Savitsky, B. Diez-Dacal, M. Philpotta, C. Bountra, H. Lingard, O. Fedorov, S. Müller, P.E. Brennan, S. Knapp, P. Filippakopoulos, RVX-208, an inhibitor of BET transcriptional regulators with selectivity for the second bromodomain, Proc. Natl. Acad. Sci. USA 110 (2013) 19754–19759.
[19] J. Wang, Z. Liu, Z. Wang, S. Wang, Z. Chen, Z. Li, M. Zhang, J. Zou, B. Dong, J. Gao, L. Shen, Targeting c-Myc: JQ1 as a promising option for c-Myc-amplified esophageal squamous cell carcinoma, Cancer Lett. 419 (2018) 64–74.
[20] S. Amemiya, T. Yamaguchi, Y. Hashimoto, T. Noguchi-Yachide, Synthesis and evaluation of novel dual BRD4/HDAC inhibitors, Bioorg. Med. Chem. 25 (14) (2017) 3677–3684.
[21] A. Heinemann, C. Cullinane, R.D. Paoli-Iseppi, J.S. Wilmott, D. Gunatilake, J. Madore, D. Strbenac, J.Y. Yang, K. Gowrishankar, J.C. Tiffen, R.K. Prinjha, N. Smithers, G.A. McArthur, P. Hersey, S.J. Gallagher, Combining BET and HDAC inhibitors synergistically induces apoptosis of melanoma and suppresses AKT and YAP signaling, Oncotarget 6 (2015) 21507–21521.
[22] J. Shahbazi, P.Y. Liu, B. Atmadibrata, J.E. Bradner, G.M. Marshall, R.B. Lock, T. Liu, The bromodomain inhibitor JQ1 and the histone deacetylase inhibitor panobinostat synergistically reduce N-Myc expression and induce anticancer effects, Clin. Cancer Res. 22 (2016) 2534–2544.
[23] G. Borbely, L.A. Haldosen, K. Dahlman-Wright, C.Y. Zhao, Induction of USP17 by combining BET and HDAC inhibitors in breast cancer cells, Oncotarget 6 (2015) 33623–33635.
[24] X. Xue, Y. Zhang, C. Wang, M. Zhang, Q. Xiang, J. Wang, A. Wang, C. Li, C. Zhang, L. Zou, R. Wang, S. Wu, Y. Lu, H. Chen, K. Ding, G. Li, Y. Xu, Benzoxazinone-containing 3,5-dimethylisoxazole derivatives as BET bromodomain inhibitors for treatment of castration-resistant prostate cancer, Eur. J. Med. Chem. 152 (2018) 542–559.
[25] Y.J. Zhao, L.C. Bai, L. Liu, D. McEachern, J.A. Stuckey, J.L. Meagher, C.Y. Yang, X. Ran, B. Zhou, Y. Hu, X.Q. Li, B. Wen, T. Zhao, S. Li, D. Sun, S.M. Wang, Structure-based discovery of 4-(6-methoxy-2-methyl-4-(quinolin-4-yl) -9h-pyrimido[4,5-b]indol-7-yl)-3,5-dimethylisoxazole (CD161) as a potent and orally bioavailable BET bromodomain inhibitor, J. Med. Chem. 60 (9) (2017) 3887–3901.
[26] D.S. Hewings, O. Fedorov, P. Filippakopoulos, S. Martin, S. Picaud, A. Tumber, C. Wells, M.M. Olcina, K. Freeman, A. Gill, A.J. Ritchie, D.W. Sheppard, A.J. Russell, E.M. Hammond, S. Knapp, P.E. Brennan, Optimization of 3,5-dimethylisoxazole derivatives as potent BET bromodomain ligands, J. Med. Chem. 56 (8) (2013) 3217–3227.
[27] J.Z. Zhang, J. Buell, K. Chan, et al. Preparation of heterocyclic compounds as BRD4 inhibitors and uses thereof, WO 2014145051, 2013-05-14.